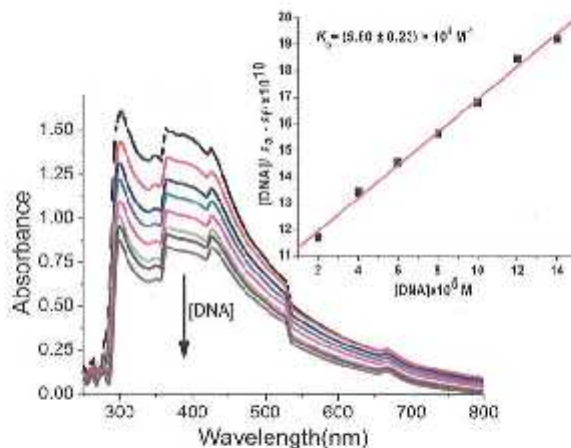


CONTENTS

1433 DNA binding, cytotoxicity and mitochondria-mediated cell apoptosis induction of a new zinc(II) complex of 5-chloro-8-hydroxyquinoline

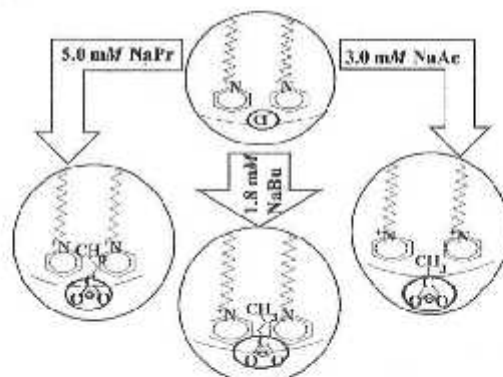
Zinc(II) complex of 5-chloro-8-hydroxyquinoline binds with ct-DNA via an intercalative mode, and also exhibits DNA cleavage activity. The complex shows lower cytotoxicity than cisplatin towards some tumor cell lines (NCI-H460, HepG2, HeLa229, T-24) and the normal liver cell line. However, in the case of the BEL-7404 liver tumor cell line, it exhibits high antitumor activity and induced apoptosis with IC_{50} value ($7.04 \pm 0.06 \mu M$) lower than that of cisplatin ($25.08 \pm 0.12 \mu M$).



Hai-Rong Zhang, Ting Meng, Qi-Pin Qin, Sheng-Ping Deng*, Qian-Qian Cao, Hong-Hua Han, Ying-Bo Li, Yun-Liang Zhang, Yan-Cheng Liu* & Hong Liang

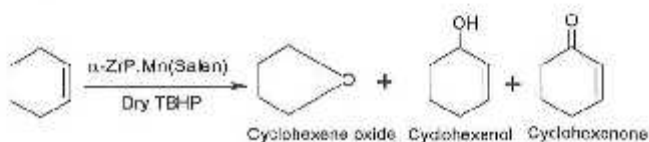
1443 Investigations on the binding behavior of competitive ions to a cationic micelle by 1H -NMR studies

Alkyl carboxylate counterions like Ac^- , Pr^- and Bu^- play a decisive role in exchange of the native counterions from CPC micelle and transform respectively to CPAc, CPPr and CPBu micelle at/or above a particular salt concentration. The overall binding nature of the added counterions on CPC micelle depends on both kosmotropy and hydrophobic effect.



1449 Catalytic oxidation of cyclohexene by α -zirconium phosphate intercalated Mn(Salen) using 70% *tert*-butylhydroperoxide as an oxidant

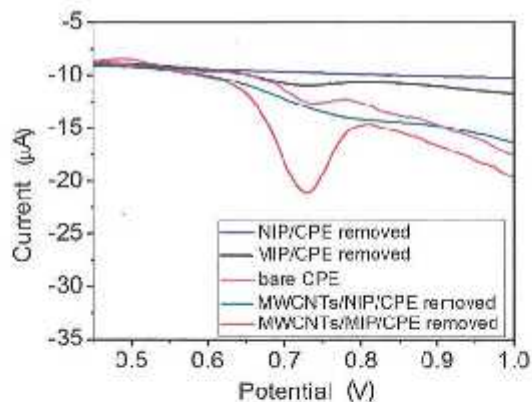
The heterogeneous catalytic system, α -ZrP.Mn(Salen)/70%TBHP, gives the maximum conversion (85%) in the oxidation of cyclohexene under the optimum conditions of 30 mmol, 10 mmol and 0.1 mmol of 70% TBHP, cyclohexene and α -ZrP.Mn(Salen), respectively at 80 °C and 6 h of reaction time. The catalyst can be reused for three cycles without appreciable loss of activity.



S Khare*, R Chokhare, P Shrivastava, J S Kirar & S Parashar

1458 Determination of the azo dye, sunset yellow, by using carbon paste electrode modified with molecularly imprinted polymer

A highly selective voltammetric sensor for sunset yellow using selective molecular imprinted polymers for preparation of carbon paste electrode is reported. The sensitivity of the sensor is improved significantly on modification with multiwalled carbon nanotubes. The MWCNTs/MIP/CPE shows very high recognition ability in comparison with the MWCNTs/NIP/CPE. Under the optimum conditions, the linear relationship between current and concentration is obtained in the range of 8×10^{-8} to 1×10^{-5} mol L⁻¹. The detection limit of the sensor is 2.667×10^{-8} mol L⁻¹ (S/N = 3).

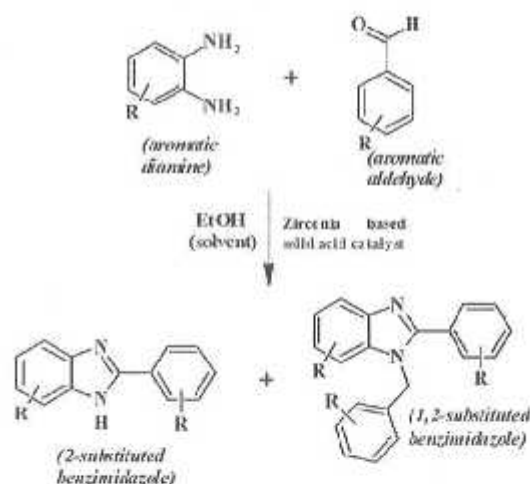


Zhihua Wang*, Yijiang Shan, Lijiang Xu, Guofan Wu & Xiaoqian Lu*

Notes

1465 Catalytic synthesis of benzimidazole derivatives over modified forms of zirconia

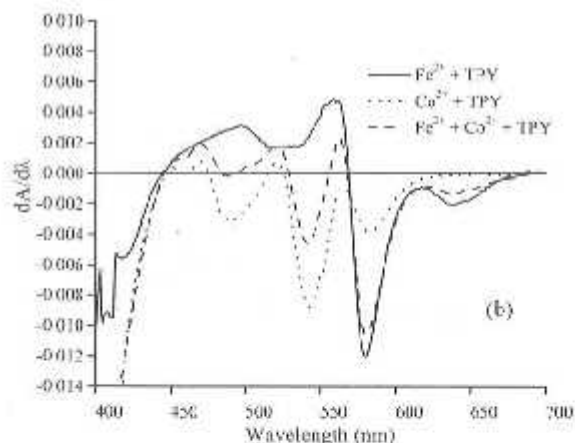
Synthesis and characterization of solid acid catalysts, viz., ZrO_2 , $Mo(VI)/ZrO_2$ and $Pt-SO_4^{2-}/ZrO_2$, is reported. $Mo(VI)/ZrO_2$ comprising moderate to strong acid sites as well as bearing the catalytically active tetragonal phase of zirconia, is an efficient and reusable solid acid catalyst for the synthesis of benzimidazoles. $Pt-SO_4^{2-}/ZrO_2$ with very strong acid sites loses its activity when reused.



T E Mohan Kumar, S Z Mohamed Shamshuddin^{*}, Venkatesh & S Reena Saritha

1471 Cloud point extraction with mixed micelles of TX-114/DOSS and derivative spectrophotometry for simultaneous determination of Fe^{2+} and Co^{2+} using 2,2',6',2''-terpyridine

A new cloud point extraction procedure with derivative spectrophotometry for the simultaneous preconcentration and determination of Fe^{2+} and Co^{2+} has been developed. Both Fe^{2+} and Co^{2+} metal ions are simultaneously complexed with 2,2',6',2''-terpyridine at a pH 3.8, and extracted into mixed micelles of Triton X-114 and docusate sodium salt. Under optimum conditions, the linear ranges of Fe^{2+} and Co^{2+} are $0.373-2.42 \mu g mL^{-1}$ and $3.14-18.86 \mu g mL^{-1}$ respectively. Their corresponding limits of detections are $0.498 ng mL^{-1}$ and $4.54 ng mL^{-1}$.



K Ravi Kumar & P Shyamala^{*}

1477 Annual Index